

# Bond Dissociations in Hypervalent Ammonium Radicals Prepared by Collisional Neutralization of Protonated Six-membered Nitrogen Heterocycles

Jill K. Wolken, Viet Q. Nguyen† and František Tureček\*

Department of Chemistry, Bagley Hall, Box 351700, University of Washington, Seattle, Washington 98195-1700, USA

Hypervalent organic ammonium radicals were generated by collisional neutralization with dimethyl disulfide of protonated 1,4-diazabicyclo[2.2.2]octane ( $1\text{H}^+$ ), *N,N'*-dimethylpiperazine ( $2\text{H}^+$ ) and *N*-methylpiperazine ( $3\text{H}^+$ ). The radicals dissociated completely on the 5.1  $\mu\text{s}$  time-scale. Radical  $1\text{H}^\cdot$  underwent competitive  $\text{N}-\text{H}$  and  $\text{N}-\text{C}$  bond dissociations producing 1,4-diazabicyclo[2.2.2]octane and small ring fragments. Dissociations of radical  $2\text{H}^\cdot$  proceeded by  $\text{N}-\text{H}$  bond dissociation and ring cleavage, whereas  $\text{N}-\text{CH}_3$  bond cleavage was less frequent. Radical  $3\text{H}^\cdot$  underwent  $\text{N}-\text{H}$ ,  $\text{N}-\text{CH}_3$  and  $\text{N}-\text{C}_{\text{ring}}$  bond cleavages followed by post-reionization dissociations of the formed cations. The pattern of bond dissociations in the hypervalent ammonium radicals derived from six-membered nitrogen heterocycles is similar to those of aliphatic ammonium radicals. © 1997 John Wiley & Sons, Ltd.

*J. Mass Spectrom.* 32, 1162–1169 (1997)

No. of Figures: 8 No. of Tables: 1 No. of Refs: 28

KEYWORDS: hypervalent ammonium radicals; neutralization–reionization mass spectrometry; diazabicyclo[2.2.2]octane; *N,N'*-dimethylpiperazine; *N*-methylpiperazine

## INTRODUCTION

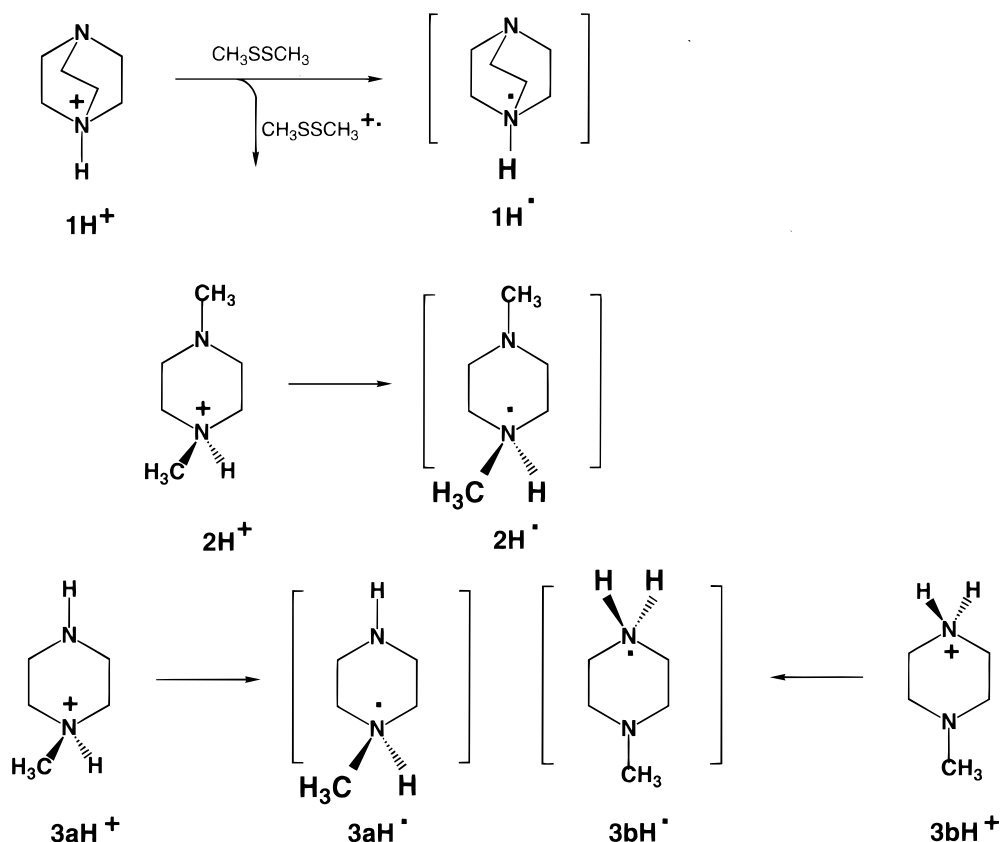
Gas-phase reduction of ammonium cations by fast collisional electron transfer produces transient ammonium radicals that formally have nine electrons at the nitrogen atom and thus violate the octet rule.<sup>1,2</sup> Hypervalent organic ammonium radicals have been generated and studied by neutralization–reionization mass spectrometry<sup>3–6</sup> (NRMS) and some of their unusual chemical properties have been elucidated. Methylammonium,<sup>7</sup> dimethylammonium,<sup>8</sup> trimethylammonium,<sup>9</sup> and pyrrolidinium radicals,<sup>10</sup> in the form of their deuterated isotopomers, were found to be metastable on the microsecond time-scale of NRMS measurements, such that small fractions of surviving radicals were detected following reionization to stable ammonium cations. The fragmentations of hypervalent ammonium radicals by  $\text{N}-\text{H}$  and  $\text{N}-\text{C}$  bond dissociations have been studied for aliphatic and aromatic systems. Methylated ammonium radicals such as methylammonium, dimethylammonium and trimethylammonium dissociate by competitive losses of  $\text{H}^\cdot$  and  $\text{CH}_3^\cdot$ , which occur, however, from different electronic states, as revealed by a recent photoexcitation study.<sup>8</sup> For example, dimethylammonium radicals in their electronic ground state are dissociative and lose predominantly  $\text{H}^\cdot$  as predicted by *ab initio* theory<sup>11</sup> and Rice–Ramsperger–Kassel–Marcus kinetic calculations.<sup>8</sup> Loss of  $\text{CH}_3^\cdot$  occurs from low excited states,

which are strongly bound with respect to  $\text{N}-\text{H}$  bond cleavage and are also responsible for the observed metastability.<sup>8</sup> Larger ammonium radicals containing combinations of hydrogen, methyl, *N*-alkyl and benzyl groups underwent dissociations by  $\text{H}$  and large alkyl or benzyl loss, whereas loss of methyl was generally weak.<sup>12,13</sup> Dissociations of quaternary ammonium radicals have also been reported.<sup>14</sup>

To elucidate the competitive bond dissociations in hypervalent organic ammonium radicals, we now report an NRMS study of cyclic systems derived from bicyclo[2.2.2]octane (1), *N,N'*-dimethylpiperazine (2) and *N*-methylpiperazine (3). These model amines all contain six-membered rings, but differ in their substitution patterns and conformational properties. For example, neutralization of cation  $1\text{H}^+$  produces a hypervalent radical ( $1\text{H}^\cdot$ ) which has only one dangling  $\text{N}-\text{H}$  bond at the hypervalent center whose cleavage could lead to direct fragmentation, whereas the  $\text{N}-\text{C}$  bonds are locked in the rigid bicyclic ring system (Scheme 1). Radical  $2\text{H}^\cdot$  has two different  $\text{N}-\text{CH}_3$  bonds and an  $\text{N}-\text{H}$  bond that can be expected to undergo dissociations to form different products. Protonation of 3 could presumably form isomeric cations  $3\text{aH}^+$  and  $3\text{bH}^+$  that produce the corresponding radicals  $3\text{aH}^\cdot$  and  $3\text{bH}^\cdot$  with two different types of dangling  $\text{N}-\text{H}$  bonds and one  $\text{N}-\text{CH}_3$  bond, which can presumably undergo competitive dissociations. The ring systems in  $2\text{H}^\cdot$  and  $3\text{H}^\cdot$  are flexible and allow for conformational transformations, which may have an effect on the neutral reactivity. We used NRMS in combination with deuterium labeling to characterize the dissociation products and deduce the leaving group abilities of the substituents in the hypervalent radicals under study.

\* Correspondence to: F. Tureček, Department of Chemistry, Bagley Hall, Box 351700, University of Washington, Seattle, Washington 98195-1700, USA.

† Present address: National Institutes of Health, Bethesda, Maryland, USA.



Scheme 1

## EXPERIMENTAL

Measurements were made on a tandem quadrupole acceleration-deceleration mass spectrometer as described previously.<sup>15</sup> Cation radicals were produced by electron ionization (EI) at sample partial pressures of  $(1-2) \times 10^{-5}$  Torr (1 Torr = 133.3 Pa). The ionization conditions were electron energy 70 eV, electron current 500  $\mu\text{A}$  and ion source temperature 180–200 °C. Ammonium cations were produced by protonation in a tight chemical ionization (CI) ion source of our design. Ammonia (Matheson, 99.99%), isobutane (Matheson, 99%) and water were used for protonations, whereas  $\text{ND}_3$  (Matheson, 99% D) and  $\text{D}_2\text{O}$  (Cambridge Isotope Laboratories, 99.9% D) were used for deuteronations. The chemical ionization gases were introduced into the ion source at apparent pressures of  $(2-4) \times 10^{-4}$  Torr as measured on a Bayard-Alpert ionization gauge located on the source diffusion pump intake. The reagent gas pressure in the ion source, estimated at 0.1–0.2 Torr, was sufficient to achieve efficient protonation and suppress electron ionization of the amines. This was monitored through the  $[\text{M} + \text{H}]^+ / [\text{M}^+]$  abundance ratios, which were  $>20$  in most instances. Collisional neutralization of 8200 eV precursor ions was carried out with dimethyl disulfide, which was introduced into the collision chamber at pressures such as to achieve 70% transmittance of the precursor ion beam. This corresponded mostly (85%) to single-collision conditions. The neutral intermediates of 5.1  $\mu\text{s}$  lifetimes were reionized by collisions with oxygen, which was admitted into the collision cell at pressures allowing 70% transmittance

of the precursor ion beam. Collisional activation of transient neutrals<sup>9</sup> was achieved by admitting helium into the differentially pumped neutral drift region at pressures such as to achieve 50% transmittance of the precursor ion beam.

Collisionally activated dissociation (CAD) spectra were obtained on a Kratos Profile HV-4 double-focusing mass spectrometer. Precursor ions were generated by  $\text{NH}_4^+ / \text{NH}_3$  or  $\text{ND}_4^+ / \text{ND}_3$  CI in a tight ion source and allowed to dissociate in a grounded collision cell that was mounted on the ion source in the first field-free region preceding the electrostatic analyzer. CAD spectra were obtained as linked B/E scans in which the magnetic field (B) and the electrostatic analyzer potentials (E) were scanned simultaneously while maintaining a constant B/E ratio. Twenty-five scans were typically acquired and averaged. Oxygen was used as a collision gas which was admitted into the collision cell at a pressure such as to allow 50% transmittance of the precursor ion beam.

1,4-Diazabicyclo[2.2.2]octane, N-methylpiperazine and N,N'-dimethylpiperazine were purchased from Aldrich and used as received. The EI mass spectra and analysis by gas chromatography/mass spectrometry revealed no impurities that would interfere with the measurements.

## RESULTS AND DISCUSSION

The formation of hypervalent radicals by collisional neutralization can be accompanied by CAD of the precursor ions that yield neutral fragments. The latter,

which are due to ion dissociations, are transmitted and reionized and thus appear in the NR mass spectra.<sup>16</sup> To identify neutral products from ion dissociations, CAD spectra of  $1\text{H}^+-3\text{D}^+$  were obtained (Table 1). The spectra and the ensuing neutral fragments are discussed together with the NR spectra for  $1\text{H}^+-3\text{D}^+$ .

Dissociations of hypervalent ammonium radicals typically proceed by simple bond cleavages to form an amine and a radical which can be identified through signature ions in the NR spectra.<sup>12</sup> Dissociations by N–H bond cleavage in  $1\text{H}^+$  would produce **1**, whose NR mass spectra were obtained for reference (Fig. 1(a) and (b)). Neutralization–reionization of stable  $1^{++}$  afforded a substantial fraction of survivor ions at  $m/z$  112, which amounted to 6.2% of the sum of the reionized peak intensities ( $\% \Sigma I_{\text{NR}}$ ). In addition to the fragments at  $m/z$  97, 84, 70, 55, 42 and 28, which are also prominent in both the EI mass spectrum of  $1^{17}$  and the CAD spectrum of  $1^{++}$ , the NR spectrum showed an abundant group of ions at  $m/z$  26–28, which corresponded to overlapping  $\text{C}_2\text{H}_x$  and  $\text{H}_x\text{CN}$  fragments (Fig. 1(a)). It is worth mentioning that the relative abundance of sur-

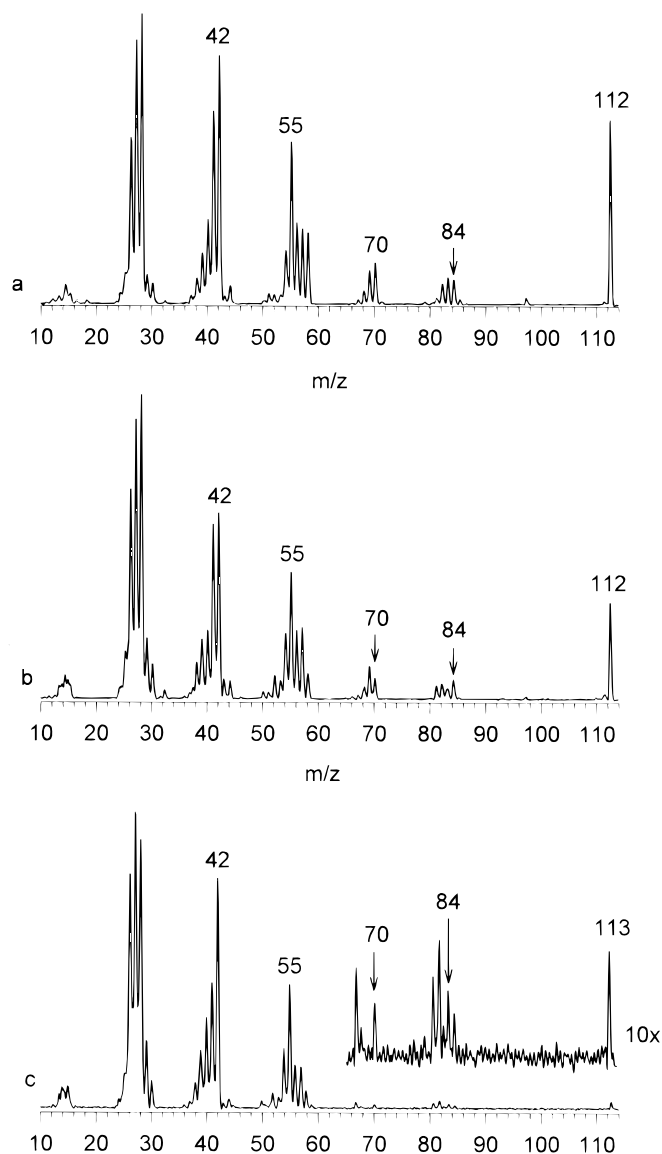


**Figure 1.** Neutralization ( $\text{CH}_3\text{SSCH}_3$ , 70% transmittance)–reionization ( $\text{O}_2$ , 70% transmittance) spectra of (a)  $1^{++}$ , and (c)  $1\text{H}^+$ . (b) Neutralization ( $\text{CH}_3\text{SSCH}_3$ , 70% transmittance)–collisional activation (He, 50% transmittance)–reionization ( $\text{O}_2$ , 70% transmittance) spectrum of  $1^{++}$ .

vivor  $1^{++}$  depended on the internal energy of the precursor ion. The NR spectrum of  $1^{++}$  prepared at  $\sim 0.1$  Torr partial pressure of **1** in the ion source, corresponding to charge-exchange self-CI conditions, showed a substantially increased survivor ion (11.9%  $\Sigma I_{\text{NR}}$ ). The energy dependence of the NR fragmentations of **1** was further investigated through neutralization–collisional activation–reionization (NCR) spectrum obtained at 50% beam attenuation due to neutral collisional activation with helium. The spectrum (Fig. 1(b)) showed survivor  $1^{++}$  of diminished relative abundance (3.4%  $\Sigma I_{\text{NR}}$ ) and increased fragments at low  $m/z$  values. The spectra thus indicated that the relative abundance of survivor  $1^{++}$  was sensitive to the internal energy content of its neutral and/or ion precursors.<sup>18</sup> This finding was important, because the survivor ion at  $m/z$  112 was a unique signature for **1**.

The NR spectrum of  $1\text{H}^+$  showed extensive dissociations (Fig. 1(c)). Weak survivor ions were observed at

**Table 1.** CAD mass spectra of  $1\text{H}^+-3\text{D}^+$

$m/z$	Relative intensity <sup>a</sup>					
	$1\text{H}^+$	$1\text{D}^+$	$2\text{H}^+$	$2\text{D}^+$	$3\text{H}^+$	$3\text{D}^+$
28	2.4				2.7	0.9
29					1.1	2.5
30					2.0	1.0
31						1.3
41	2.0				1.5	0.9
42	4.0		4.7	4.0	5.1	3.4
43	1.4		3.3	1.8	3.3	2.3
44	2.1		9.3	0.9	11.9	3.1
45				3.8		9.1
46						4.2
54	2.0				0.9	
55	5.3	4.2			1.1	0.9
56	12.3	3.8	1.6	0.9	5.5	1.5
57	3.3	9.6	3.2	1.7	5.3	5.0
58	5.3	1.4	28.8	5.8	34.1	6.2
59		1.9		22.1	1.8	25.7
60						6.5
68	1.4					
69	1.8					
70	18.9	9.3	14.7	13.3	6.4	5.9
71	0.9	18.2	14.9	11.1	1.4	1.6
72			4.6	7.6	1.0	1.1
73				1.1		1.1
82	3.2	0.8				
83	5.4	3.6			1.0	
84	15.3	22.0			1.3	0.8
85	2.1	12.9	1.4	0.9	1.0	1.1
86			1.6	2.5		1.5
97	4.4					
98	1.3	7.4	0.9			
99			0.8	1.7	5.1	
100				1.0		4.3
111	2.4					
112		2.9				
113			10.2	15.6		
114				3.0		

<sup>a</sup> Relative to the sum of fragment ion peak intensities,  $\% \Sigma I_{\text{CAD}}$ . Peaks below 0.8  $\% \Sigma I_{\text{CAD}}$  were included in  $\Sigma I_{\text{CAD}}$  but are not listed here.

$m/z$  113; however, these peaks were not completely reproducible over seven multi-scan measurements taken over a period of several months. The peaks at the apparent  $m/z$  of  $1\text{H}^+$  may well be due to the  $^{13}\text{C}$  and  $^{15}\text{N}$  isotopomers of residual  $1^{+\cdot}$  that overlap by mass with  $1\text{H}^+$ . Previous work on hypervalent ammonium radicals has shown that amine cation radicals had substantially greater NR efficiencies than did ammonium cations, so that contamination by amine isotopomers was of concern.<sup>8,9</sup> Hence the existence of metastable  $1\text{H}^+$  has not been safely established.

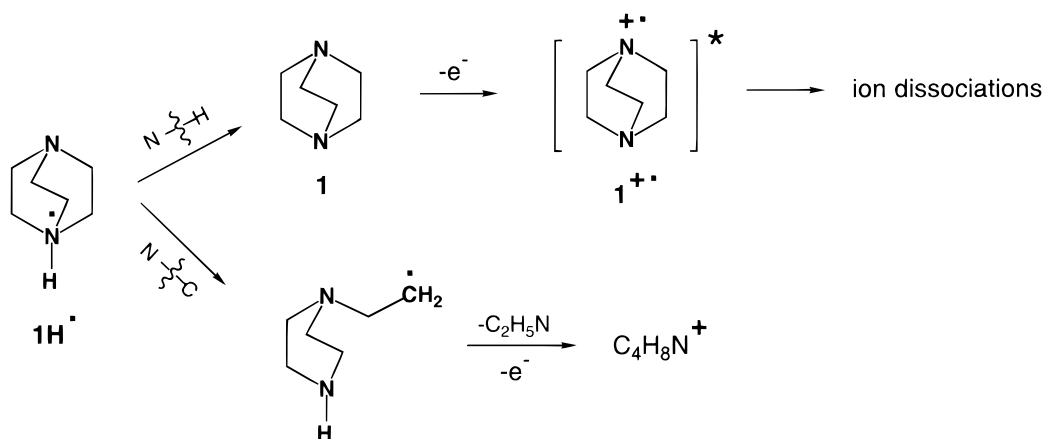
The NR dissociations of  $1\text{H}^+$  produced abundant low-mass fragments, e.g. the  $\text{C}_2\text{H}_x$  and  $\text{H}_x\text{CN}$  group at  $m/z$  26–28, the  $\text{C}_2\text{H}_x\text{N}$  group at  $m/z$  38–44 and the  $\text{C}_3\text{H}_x\text{N}$  group at  $m/z$  54–58. To identify possible contamination in the NR spectra by neutral fragments from CAD of precursor ions, the CAD spectra of  $1\text{H}^+$  and  $1\text{D}^+$  were obtained. These showed ion dissociations yielding  $\text{CH}_4$ ,  $\text{C}_2\text{H}_5$ ,  $\text{C}_2\text{H}_5\text{N}$  and  $\text{C}_3\text{H}_7\text{N}$  as neutral counterparts. The first three of these were negligible in the NR spectra of  $1\text{H}^+$ , whereas  $\text{C}_3\text{H}_7\text{N}$  appeared with moderate relative abundance and can be due in part to precursor ion dissociations. The comparison of the CAD and NR spectra thus showed clearly that CAD of the precursor ions was a minor process.

The NR fragmentations depended slightly on the internal energy of the  $1\text{H}^+$  precursor ions when prepared by protonations with  $\text{H}_3\text{O}^+$ ,  $t\text{-C}_4\text{H}_9^+$ ,  $\text{NH}_4^+$  and self-CI of decreasing exothermicity. The fragments obtained from  $1\text{H}^+$  coincided with those in the NR spectrum of  $1^{+\cdot}$  (Fig. 1(a)). However, the signature peak of reionized  $1^{+\cdot}$  was absent in the NR spectra of  $1\text{H}^+$ . The NR spectra of  $1\text{D}^+$ , prepared by deuteration with  $\text{ND}_4^+$  and  $\text{D}_3\text{O}^+$ , showed no survivor ions (spectra not shown). Interestingly, the fragment groups at  $m/z$  54–58 and 38–44 showed no significant mass shifts due to the presence of deuterium. Mass shifts due to deuterium retention were observed for  $\text{HC}\equiv\text{ND}^+$  at  $m/z$  29 and the small peak at  $m/z$  71, which was due to loss of  $\text{C}_2\text{H}_5\text{N}$ .

The product analysis and deuterium labeling data allow for the following interpretation (Scheme 2). The  $1\text{H}^+$  and  $1\text{D}^+$  radicals formed by collisional neutralization of their cations are unstable on the 5  $\mu\text{s}$  time-scale of the experiment. This result is consistent with the previous studies of hypervalent ammonium radicals derived from tertiary amines.<sup>9,10,12,13</sup> Although no

energy data are available for  $1\text{H}^+$ , previous ab initio calculations on the related trimethylammonium suggested that the radical was unbound with respect to N–H bond cleavage.<sup>9,11</sup> The absence of deuterium in the  $\text{C}_2\text{H}_x\text{N}$  and  $\text{C}_3\text{H}_x\text{N}$  fragments suggested cleavage of the N–H bond in  $1\text{H}^+$  forming **1**, which was an apparent contradiction with the absence of reionized  $1^{+\cdot}$  in the NR spectrum of  $1\text{H}^+$ . These data can be reconciled by assuming that the loss of H from  $1\text{H}^+$  is highly exothermic<sup>8,9,11</sup> and results in vibrational excitation in the neutral intermediate **1**. Reionization of the latter, which is also accompanied by internal energy deposition,<sup>18,19</sup> thus produces a vibrationally excited cation radical, which dissociates by ring-cleavage fragmentations. The energy dependence of  $1^{+\cdot}$  dissociations upon NCR is consistent with this interpretation. The retention of deuterium in  $\text{HC}\equiv\text{NH}^+$  indicates ring cleavage in  $1\text{H}^+$ . The intermediates of the N–C bond cleavage in  $1\text{H}^+$  are radicals, which are likely to undergo further ring-cleavage dissociations to form small stable fragments, as observed. One such intermediate, due to loss of  $\text{C}_2\text{H}_5\text{N}$ , was detected as a small peak at  $m/z$  70 (Fig. 1(c)), which retained the deuterium atom when formed from  $1\text{D}^+$ . It can be concluded that  $1\text{H}^+$  undergoes both N–H and N–C bond cleavages as summarized in Scheme 2. However, the branching ratio of these dissociations is difficult to obtain from the spectral data owing to the internal energy effects and lack of unique signature ions.

The internal energy effects on the NR dissociations of  $1^{+\cdot}$  deserve a brief comment. The electronic states in **1** were studied previously by Bernstein and co-workers and a  $(2p)^2 \rightarrow (2p3s)$  Rydberg state of 1.8  $\mu\text{s}$  lifetime was identified at 4.44 eV above the  $^1\text{A}_1$  ground state.<sup>20–22</sup> Vertical ionization of **1** can occur from the highest occupied  $n_+$  orbital, which corresponds to a combination of the lone-pair orbitals centered on the nitrogen atoms.<sup>23</sup> The adiabatic ionization energy of **1**,  $\text{IE}_a = 7.197$  eV,<sup>22</sup> is 0.32 eV below the vertical ionization energy.<sup>23</sup> Hence, the Franck–Condon effects (31 kJ mol<sup>-1</sup>) that can contribute to internal energy deposition in  $1^{+\cdot}$  upon vertical ionization and in **1** upon vertical neutralization are only moderate. The first excited state in  $1^{+\cdot}$  lies 2.13 eV above the ground state and is probably dissociative by analogy with the excited states in aliphatic amines.<sup>18</sup> The energy data indicate that electronic excitation in **1** and  $1^{+\cdot}$  should lead to



Scheme 2

rapid dissociations, whereas the Franck–Condon energies alone should not. The complete dissociation of **1** and/or  $1^{+}$ , when produced by the reaction sequence  $1H^{\cdot} \rightarrow 1 \rightarrow 1^{+}$ , thus could possibly be due to the formation of electronically excited states in the neutral intermediate **1** or in reionized  $1^{+}$ .

Hypervalent radical  $2H^{\cdot}$  derived from protonated *N,N'*-dimethylpiperazine ( $2H^{+}$ ) can dissociate by competitive cleavages of the N–H, N–CH<sub>3</sub> and N–C<sub>ring</sub> bonds. The former two dissociations would yield stable neutral products, **2** and **3**, respectively, whose NR spectra were recorded for reference (Fig. 2). The NR spectrum of  $2^{+}$  showed pronounced fragment peaks but gave a negligible survivor ion at  $m/z$  114 (Fig. 2(a)). This contrasts with EI, which produces an abundant molecular ion  $2^{+}$  (50% of the C<sub>2</sub>H<sub>5</sub>N<sup>+</sup> base peak) in the 70 eV EI mass spectrum.<sup>17</sup> The C<sub>4</sub>H<sub>9</sub>N<sup>+</sup> fragment at  $m/z$  71, which was due to ring cleavage and loss of CH<sub>2</sub>=NCH<sub>3</sub>, provided a unique signature peak for **2**. The NR spectrum of  $3^{+}$  showed a very weak survivor ion at  $m/z$  100 (Fig. 2(b)). Ring cleavage<sup>24</sup> resulted in a prominent C<sub>3</sub>H<sub>8</sub>N<sup>+</sup> fragment at  $m/z$  58,<sup>25</sup> which was used as a signature for **3**. It should be noted, however, that the NR spectrum of  $2^{+}$  also showed a small peak

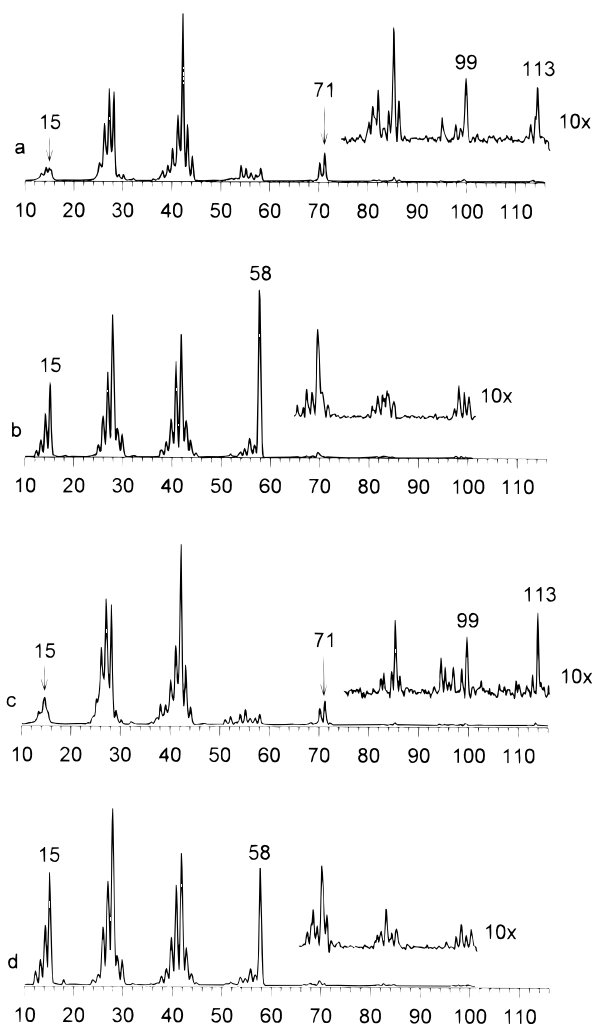


**Figure 2.** Neutralization–reionization spectra of (a)  $2^{+}$  and (b)  $3^{+}$ . Neutralization–collisional activation–reionization spectra of (c)  $2^{+}$  and (d)  $3^{+}$ . Collision conditions as in Fig. 1.

at  $m/z$  58 (Fig. 2(a)), which therefore was not unique for **3**. The NR spectra of both  $2^{+}$  and  $3^{+}$  displayed peaks of CH<sub>3</sub><sup>+</sup> which had different relative abundances (Fig. 2(a) and (b)). Collisional activation of neutral **2** resulted in a slightly increased formation of small fragments, e.g. CH<sub>3</sub><sup>+</sup>, C<sub>2</sub>H<sub>x</sub><sup>+</sup> and CH<sub>x</sub>N<sup>+</sup> at  $m/z$  24–30 and C<sub>2</sub>H<sub>x</sub>N<sup>+</sup> at  $m/z$  38–44 (Fig. 2(c)). However, the signature peak of C<sub>4</sub>H<sub>9</sub>N<sup>+</sup> at  $m/z$  71 did not decrease appreciably. Collisional activation of neutral **3** resulted in a substantially increased formation of low-mass fragments, but did not impair observation of the signature C<sub>3</sub>H<sub>8</sub>N<sup>+</sup> ion at  $m/z$  58 (Fig. 2(d)).<sup>25</sup>

The NR spectrum of  $2H^{+}$  from protonation with NH<sub>4</sub><sup>+</sup> showed no survivor ion and several groups of fragments at  $m/z$  70–72, 50–58, 38–44, 25–30 and 13–15 (Fig. 3). Neutral products from CAD of precursor ions  $2H^{+}$  were identified by comparing the CAD and NR spectra (Table 1 and Fig. 3). CAD of  $2H^{+}$  produced H<sub>2</sub>, C<sub>2</sub>H<sub>6</sub>N, C<sub>2</sub>H<sub>7</sub>N and C<sub>3</sub>H<sub>7</sub>N as the complementary neutral fragments. However, with the exception of C<sub>2</sub>H<sub>6</sub>N<sup>+</sup> at  $m/z$  44 (Fig. 3), these were weak in the NR spectrum, attesting to the inefficiency of CAD compared with collisional neutralization.

The signature peak in the NR spectrum of C<sub>4</sub>H<sub>9</sub>N<sup>+</sup> at  $m/z$  71 pointed to the formation of **2** (see above). However, the peak of C<sub>3</sub>H<sub>8</sub>N<sup>+</sup> at  $m/z$  58 was weak, indicating an inefficient loss of methyl to form **3**. No survivor ion was observed in the NR spectrum of  $2H^{+}$  from the more exothermic protonation with H<sub>3</sub>O<sup>+</sup>. This spectrum (not shown) displayed the  $m/z$  71 signature ion of **2**, while the  $m/z$  58 signature of **3** was very weak. NR of  $2D^{+}$  from deuteration with ND<sub>4</sub><sup>+</sup> showed no mass shift for the  $m/z$  71 peak, consistent with loss of D, and an  $m/z$  58 →  $m/z$  59 shift indicating retention of deuterium and loss of CH<sub>3</sub>. No survivor  $2D^{+}$  ion was detected. The fragments observed for  $2H^{+}$  do not exclude an initial N–C<sub>ring</sub> bond cleavage. Unfortunately, the presumed intermediates of such ring-cleavage dissociations are unstable radicals for which we had no reference spectra. It is also conceivable that further dissociations of such ring-opened intermediates would be indistinguishable by product analysis from the post-reionization ring fragmentations of  $2^{+}$  and  $3^{+}$  (Scheme 3).

Protonation of **3** with NH<sub>4</sub><sup>+</sup> could proceed exothermically at both the secondary and tertiary amine

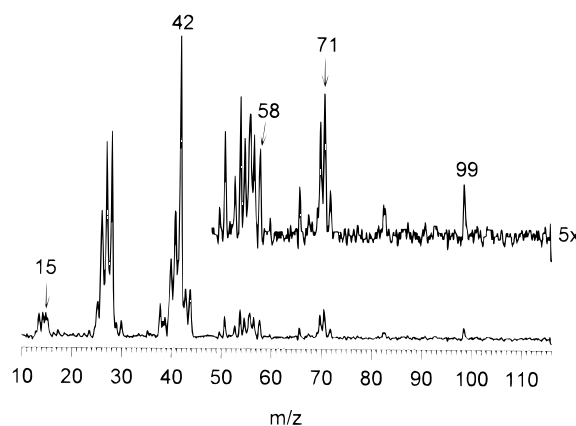
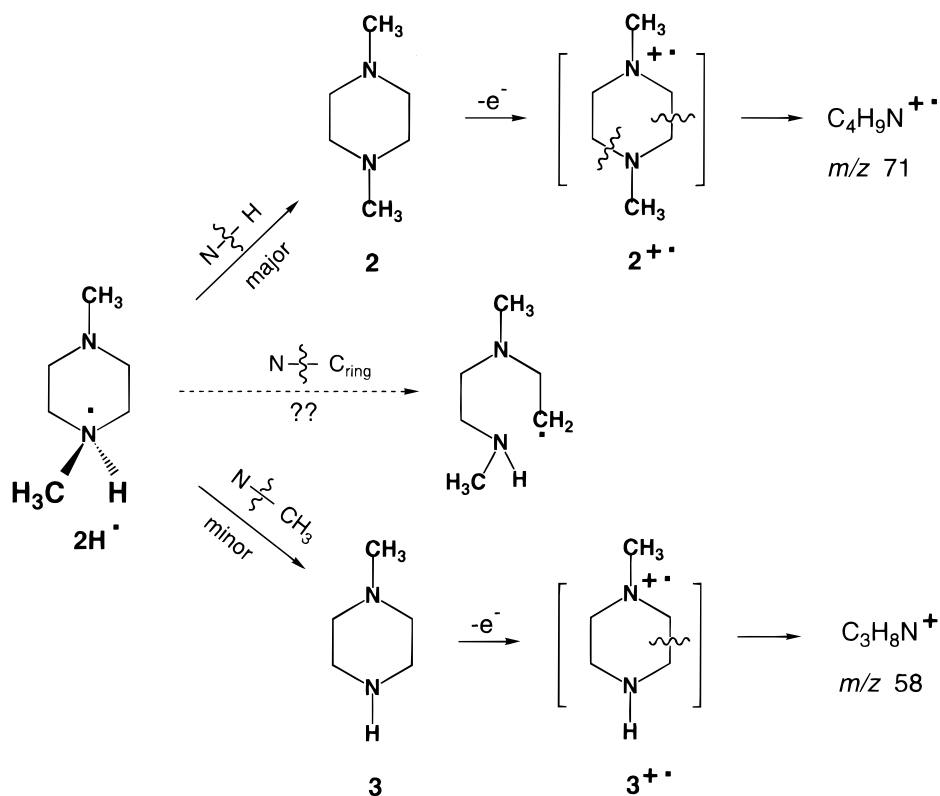


**Figure 3.** Neutralization–reionization spectrum of  $2H^{+}$ . Collision conditions as in Fig. 1.

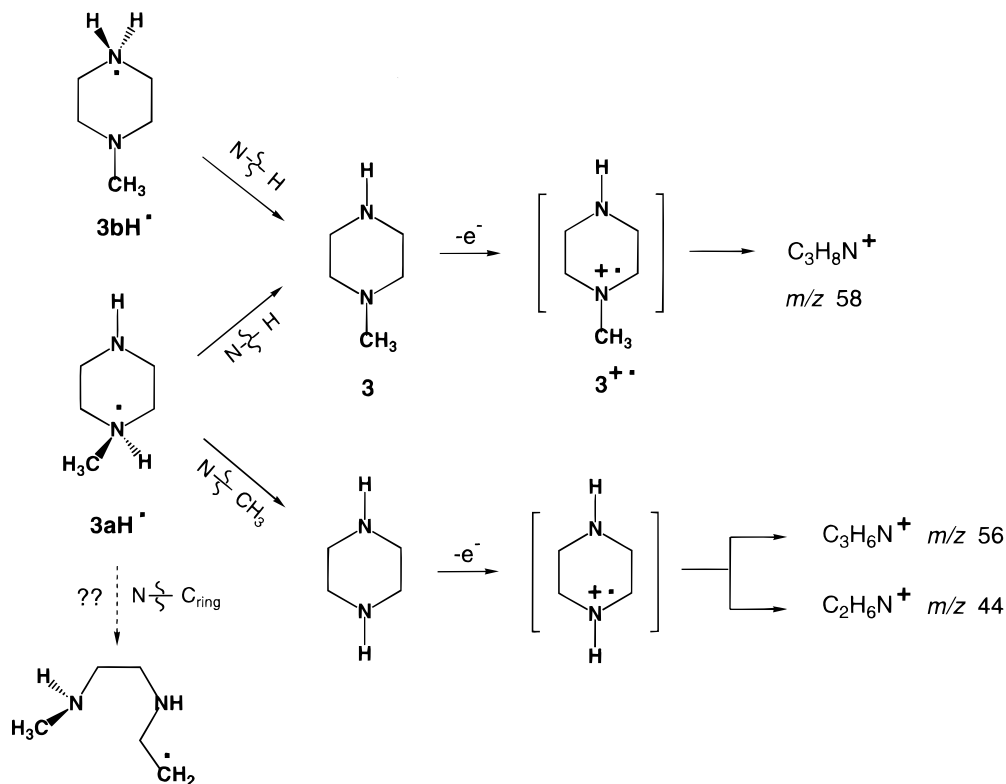


Scheme 3.

groups<sup>26–28</sup> to produce a mixture of isomeric ions  $3aH^+$  and  $3bH^+$ , respectively. No attempt at distinguishing these isomers was made and the ions are hereinafter referred to as  $3H^+$ . The NR spectrum of  $3H^+$  is shown in Fig. 4(a). To distinguish the possible neutral fragments from CAD of  $3H^+$ , the CAD and NR spectra were compared (Table 1 and Fig. 4(a)). CAD of

$3H^+$  produced two major neutral fragments, e.g.  $C_2H_5N$  and  $C_3H_7N$  (Table 1). However, these were very weak in the NR spectrum of  $3H^+$  (cf.  $m/z$  43 and 57, Fig. 4(a)), confirming that CAD concomitant with collisional neutralization was inefficient.

The survivor ion of  $3H^+$  was absent in the NR spectrum, whereas the signature  $C_3H_8N^{+\cdot}$  fragment at  $m/z$



Scheme 4.

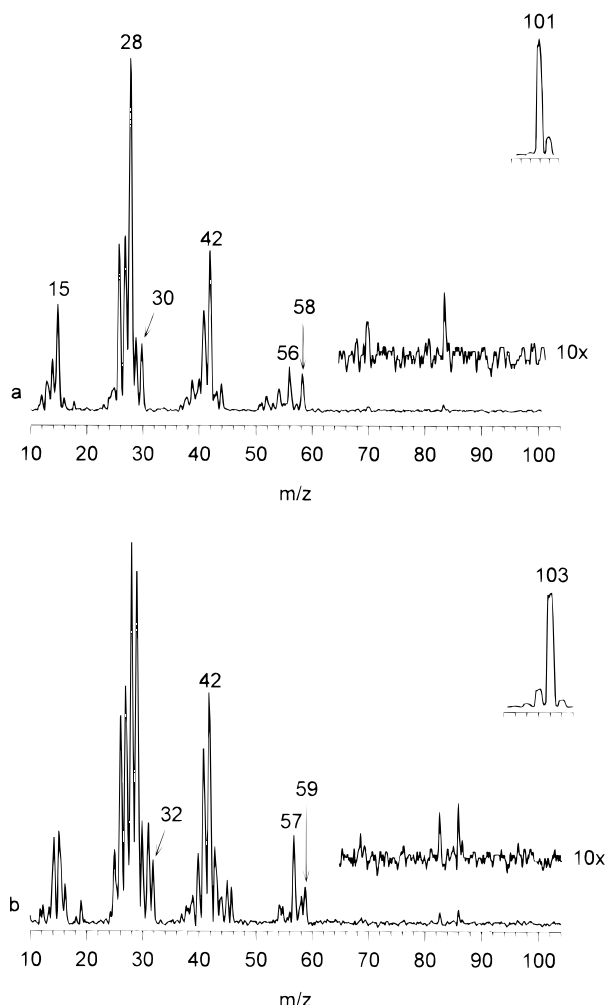


**Figure 4.** Neutralization–reionization spectra of (a)  $3\text{H}^+$  and (b)  $3\text{D}^+$ . The insets show the  $3\text{H}^+$  and  $3\text{D}^+$  ion abundances in the  $\text{NH}_4^+$  and  $\text{ND}_4^+$  chemical ionization spectra. Collision conditions as in Fig. 1.

58 indicated loss of  $\text{H}^{\cdot}$  to form **3**. However, the spectrum also showed peaks at  $m/z$  56 and 44, which were indicative of loss of methyl to form piperazine. Piperazine shows abundant  $\text{C}_3\text{H}_6\text{N}^+$  and  $\text{C}_2\text{H}_6\text{N}^+$  fragments at  $m/z$  56 and 44, respectively, in its EI mass spectrum.<sup>17</sup>

The survivor ion was also absent in the NR spectrum of  $3\text{D}^+$  from deuteration with  $\text{ND}_4^+$  (Fig. 4(b)). The spectrum showed mass shifts of  $m/z$  58  $\rightarrow$   $m/z$  59 and  $m/z$  56  $\rightarrow$   $m/z$  57, which were consistent with the ring fragmentation mechanisms in reionized  $3^{+\cdot}$  and piperazine $^{+\cdot}$ , respectively (Scheme 4). Retention of both deuterium atoms in a fraction of dissociating  $3\text{H}^{\cdot}$  was

apparent from the mass shift of the  $\text{C}_2\text{H}_6\text{N}^+$  ion from  $m/z$  44 to  $m/z$  46. This may be interpreted by a loss of methyl or an  $\text{N}-\text{C}_{\text{ring}}$  bond cleavage in  $3\text{H}^{\cdot}$  followed by a ring fragmentation (Scheme 4). Note that regardless of the  $\text{C}_2\text{H}_6\text{N}^+$  ion structure and mechanism of its formation, the dissociation mandates a hydrogen transfer to occur. However, hydrogen transfer also occurs in the ring fragmentations of the piperazine cation radical that may be formed by loss of methyl from  $3\text{H},\text{D}^{\cdot}$  followed by reionization. Hence a ring opening in  $3\text{H}^{\cdot}$  to form a radical intermediate and the loss of methyl to form piperazine were not distinguished unambiguously by the present labeling data.

## CONCLUSIONS

Collisional neutralization of ammonium ions derived from protonated 1,4-diazabicyclo[2.2.2]octane,  $\text{N},\text{N}'$ -dimethylpiperazine and  $\text{N}$ -methylpiperazine resulted in the formation of hypervalent ammonium radicals that dissociated completely on the 5  $\mu\text{s}$  time-scale. In contrast to methylammonium, dimethylammonium and pyrrolidinium, no microsecond metastability was observed for  $\text{N}$ -deuterated cyclic ammonium radicals from the six-membered heterocycles under study.  $\text{N}-\text{H}$  bond cleavage was observed for all three types of hypervalent radicals and represented a universal dissociation pathway. This finding was consistent with the previous theoretical and experimental studies of alkyl and benzylammonium radicals. Dissociations of  $\text{N}-\text{C}_{\text{ring}}$  bonds also took place, although their unambiguous identification was made difficult by overlapping dissociations of reionized fragments. Loss of methyl was inefficient in  $\text{N},\text{N}'$ -dimethylpiperazinium, but competed with loss of  $\text{H}^{\cdot}$  from  $\text{N}$ -methylpiperazinium. The nature of this peculiar effect is not well understood at present. However, a similar effect was observed previously for methyl loss from hypervalent  $\text{N},\text{N}$ -dimethyl and  $\text{N}$ -methylbenzylammonium radicals and hence it may represent a general fragmentation characteristics of these unusual transient species.

## Acknowledgements

Generous support of this work by a grant from the National Science Foundation (CHE-9412774) is gratefully acknowledged. We also thank Dr Martin Sadílek and Aaron Frank for technical assistance.

## REFERENCES

- G. N. Lewis, *J. Am. Chem. Soc.* **38**, 762 (1916).
- A. E. Reed and P. v. R. Schleyer, *J. Am. Chem. Soc.* **112**, 1434 (1990).
- J. L. Holmes, *Mass Spectrom. Rev.* **8**, 513 (1989).
- F. W. McLafferty, *Int. J. Mass Spectrom. Ion Processes* **118/119**, 221 (1992).
- F. Tureček, *Org. Mass Spectrom.* **27**, 1087 (1992).
- N. Goldberg and H. Schwarz, *Acc. Chem. Res.* **27**, 347 (1994).
- A. B. Raksit, S.-J. Jeon and R. F. Porter, *J. Phys. Chem.* **90**, 2298 (1986).
- V. Q. Nguyen, M. Sadílek, A. J. Frank, J. G. Ferrier and F. Tureček, *J. Phys. Chem. A*, **101**, 3789 (1997).
- S. A. Shaffer and F. Tureček, *J. Am. Chem. Soc.* **116**, 8647 (1994).
- L. Frösing, J. K. Wolken, F. Tureček and V. Q. Nguyen, in *Proceedings of the 44th ASMS Conference on Mass Spectrometry and Allied Topics*, Portland, OR, 1996, p. 95.

11. A. I. Boldyrev and J. Simons, *J. Chem. Phys.* **97**, 6621 (1992).
12. S. A. Shaffer, M. Sadilek and F. Tureček, *J. Org. Chem.* **61**, 5234 (1996).
13. S. A. Shaffer and F. Tureček, *J. Am. Soc. Mass Spectrom.* **6**, 1004 (1995).
14. S. Beranová and C. Wesdemiotis, *Int. J. Mass Spectrom. Ion Processes* **134**, 83 (1994).
15. F. Tureček, M. Gu and S. A. Shaffer, *J. Am. Soc. Mass Spectrom.* **3**, 493 (1992).
16. M. J. Polce, S. Beranova, M. J. Nold and C. Wesdemiotis, *J. Mass Spectrom.* **31**, 1073 (1996).
17. F. W. McLafferty and D. B. Stauffer, *The Wiley/NBS Registry of Mass Spectral Data*, pp. 23, 48, 82, 95. Wiley, New York (1989).
18. V. Q. Nguyen and F. Tureček, *J. Mass Spectrom.* **31**, 843 (1996).
19. S. Beranová and C. Wesdemiotis, *J. Am. Soc. Mass Spectrom.* **5**, 1093 (1994).
20. D. H. Parker and P. Avouris, *J. Chem. Phys.* **71**, 1241 (1979).
21. Q. Y. Shang, P. O. Moreno, S. Li and E. R. Bernstein, *J. Chem. Phys.* **98**, 1876 (1993).
22. Q. Y. Shang, P. O. Moreno and E. R. Bernstein, *J. Am. Chem. Soc.* **116**, 302 (1994).
23. E. Heilbronner and K. A. Muszkat, *J. Am. Chem. Soc.* **92**, 3818 (1970).
24. F. W. McLafferty and F. Tureček, *Interpretation of Mass Spectra*, 4th edn. University Science Books, Mill Valley, CA (1993).
25. S. A. Shaffer, F. Tureček and R. L. Cerny, *J. Am. Chem. Soc.* **115**, 12117 (1993).
26. From the proton affinities (kJ mol<sup>-1</sup>) of ammonia (853), piperidine (947), piperazine (938) and N-methylpiperidine (961), see Refs 27 and 28.
27. J. A. Szulejko and T. B. McMahon, *J. Am. Chem. Soc.* **115**, 7839 (1993).
28. S. G. Lias, J. F. Liebman and R. D. Levin, *J. Phys. Chem. Ref. Data* **13**, 695 (1984).